Applied Acoustics 88 (2015) 137–145

Contents lists available at ScienceDirect

Applied Acoustics

journal homepage: www.elsevier.com/locate/apacoust

Prediction of sound field from recoilless rifles in terms of source decomposition

Byunghak Kong [a], Kyuho Lee [a], Seo-Ryong Park [a], Seokjong Jang [a], Soogab Lee [b,*]

[a] Department of Mechanical and Aerospace Engineering, Seoul National University, Seoul 151-742, Republic of Korea
[b] Center for Environmental Noise and Vibration Research, Engineering Research Institute, Department of Mechanical and Aerospace Engineering, Seoul National University, Seoul 151-742, Republic of Korea

ARTICLE INFO

Article history:
Received 11 November 2013
Received in revised form 30 April 2014
Accepted 21 August 2014
Available online 16 September 2014

Keywords:
Hybrid prediction model
Recoilless rifle
Muzzle blast
Jet noise

ABSTRACT

In the present study, sound field from M40A1, a type of recoilless rifles, was measured using sound analyzers. Contrary to expectations based on the common characteristics of muzzle blast in previous studies, significantly different waveforms compared to those in other directions were observed in each acoustic pressure signal. In order to clarify how the surroundings affected the sound field, the temporal, spectral and directional characteristics were investigated using correlation functions and Fourier transforms. As a result, additional sources near the rear nozzle of the weapon were identified. Under the operating circumstances of recoilless weapons, blast and jet noise sources were found to be consistent with their acoustical characteristics. A hybrid model integrating the influences of blast and jet noise identified from source decomposition was derived according to the ISO standard 17201 and NASA empirical formulae. Since the predicted directivity pattern agrees moderately well with that measured in previous and present studies and the spectral distributions are in accordance with the measured ones, the hybrid model proposed in this study is considered to be appropriate for predicting the sound field from M40A1 recoilless rifle.

1. Introduction

Muzzle blast, a type of impulse sound, is a phenomenon associated with the rapid discharge of compressed air and propellant gas, which displace the ambient air and form blast waves at the front of the spherical volume of the gases [1]. These shock fronts contribute to huge variations in the local acoustic pressure within a very short time during propagation. This is a major characteristic that describes the acoustical similarity of muzzle blast and is called impulsiveness, which is revealed by the presence of several acoustical features such as short duration time, nonlinearity near the source, and broadband noise [2].

Most studies of muzzle blast [3–15] are based on this similarity of the impulsiveness. Weber [3,4] developed a blast source model to describe the strength and spectrum of the blast noise for an explosion in air depending on the radius of a spherical volume of compressed gas, and the International Organization for Standardization (ISO) [5,6] has recommended procedures to estimate the source data with respect to the energy, direction, and frequency contents using the Weber radius and provides guidance for calculating the sound propagation from shooting ranges. In addition, Fansler et al. [7,8] proposed a scaling law to predict the blast wave overpressure levels from an arbitrary gun muzzle according to dimensionless parameters such as the scaling length, Mach disc location, and blow-down parameter in a perspective on damage risk to the human body. Likewise, an optical measurement of the muzzle flow field by Schmidt and Shear [9], numerical simulations using a remarkable source model by Bin et al. [10] and Jiang [11–14], and a theoretical approach by Erdos and Del Guidice [15] also investigated its physical mechanism and characteristics based on these similarities.

In this study, the characteristics of shooting range from M40A1 recoilless rifle were investigated by acoustic pressure signals based on the principle of these similarities [16]. Typically, the recoil force is induced as a reaction to the propelling force that accelerates the projectile when a weapon is firing, and it has an impact on an operator. However, M40A1 becomes recoilless by cancellation of the recoil force, so this force rarely affects the user. Hence, there might be significant changes in the acoustic features that can enable "recoil" and "recoilless" rifles to be distinguished by means of the similarities in impulsiveness.

* Corresponding author. Address: #311-105 Seoul National University, 1 Gwanak-ro, Gwanak-gu, Seoul 151-742, Republic of Korea. Tel.: +82 2 880 7384.
E-mail address: solee@snu.ac.kr (S. Lee).

http://dx.doi.org/10.1016/j.apacoust.2014.08.012
0003-682X/

Accordingly, the sound field was measured to investigate the similarities and dissimilarities of M40A1, and a prediction model that can include the effects of the dissimilarities is proposed. This article first presents an ISO standard procedure, which is one of prediction methods for shooting range based on the similarity, and introduces the measurement conditions in Section 2. Subsequently, the acoustic properties of muzzle blast from M40A1 are examined using measured signals, and the remarkable differences from recoil weapons are analyzed in Section 3. Then, a hybrid prediction model is suggested, and its accuracy and validity are examined in Section 4.

2. Methodologies

2.1. ISO 17201

Parts 2 and 3 of the international standard series ISO 17201 cover the prediction of source data and propagation of shooting noise, and they ultimately specify methods for the calculation of the sound exposure level (SEL) at a certain receiver point from muzzle blast. These procedures are briefly described in Fig. 1.

In order for the source data to be used as input variables for further calculation, the data must be frequency and angle dependent because the acoustic energy and spectrum of muzzle blast are highly directional. Thus, ISO 17201 Part 2 recommends a procedure that is consistent with this requirement. This method has two major steps: estimation of the acoustic energy and calculation of the spectrums including their directional characteristics. The former step, acoustic energy estimation, is based on a similarity principle that implies that a part of chemical energy generated from the explosion of the propellant is used to accelerate a projectile. In the first, the kinetic energy of the projectile is calculated from its mass and launch speed, and the chemical energy is estimated from the projectile energy by the recommended conversion factor. Then, the total acoustic energy of the muzzle blast is calculated from the conversion ratios between energy types. In the second, the directivity of the source is applied according to the type of weapon, e.g., rifle, pistol, and shotgun, as shown in Fig. 1, and finally, the angular source energy distribution is obtained as follows [5]:

$$S_q(\alpha) = \frac{p_W^2}{\rho_c} 4\pi R_W^2 \int_{\omega_1}^{\omega_2} \frac{1}{\pi} \left[\omega^2 + 9\frac{c^2}{R_W^2}\left(\frac{c^2}{R_W^2\omega^2}+1\right)\right]^{-1} d\omega \quad (1)$$

In Part 3, the SEL at the reception point from one specific shot is calculated using a ray tracing model. In this step, the sound power level and directivity have to be replaced by the angular sound source distribution estimated in Part 2, and the propagation conditions such as geometric spreading, atmospheric absorption, and ground reflection are imposed. Therefore, the SEL, $L_E(f)$, can be obtained using the following equation [6]:

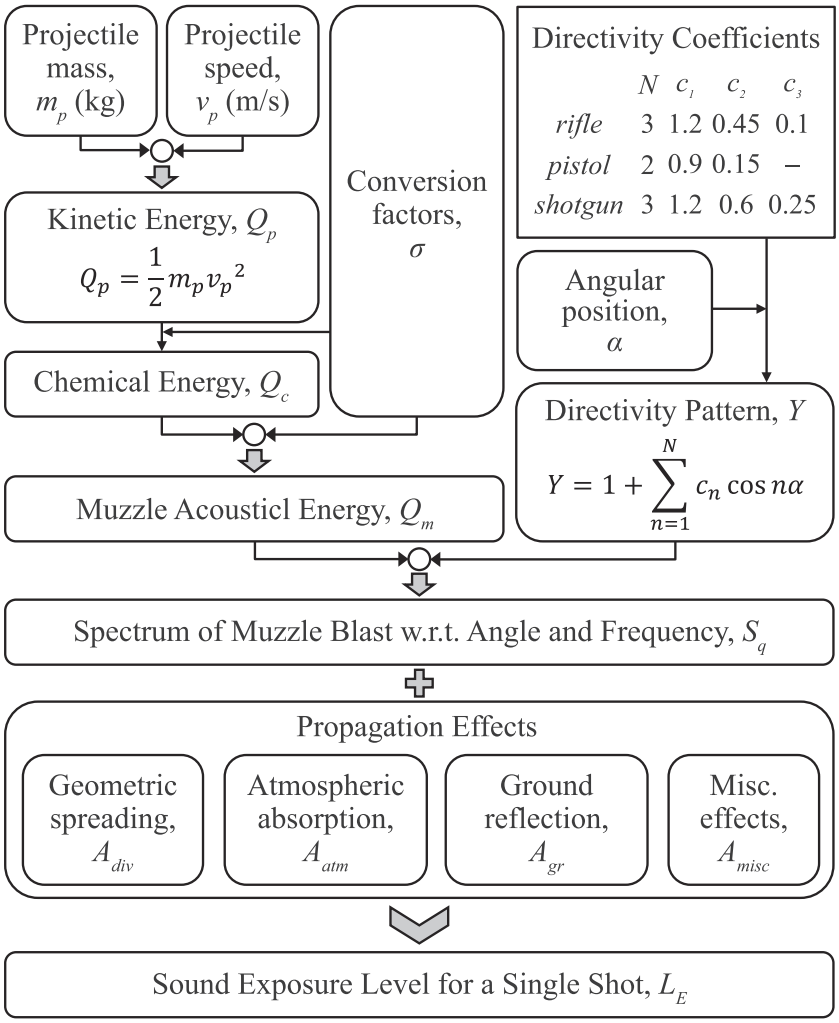

Fig. 1. ISO 17201: Flow chart of the estimation procedure for sound exposure level from the muzzle blast [5,6].

$$L_E(f) = L_q(\alpha,f) - A_{div}(r) + 11\ \text{dB} - A_{atm}(r,f) - A_{gr}(r,f) - A_{misc}(r,f) \quad (2)$$

In Eq. (2), L_q, A_{div}, A_{atm}, and A_{gr} indicate the angular source energy distribution, a correction for the geometric spread, the air absorption, and the ground effect, respectively, and A_{misc} includes other effects such as the meteorological conditions. These terms are calculated according to ISO 9613 [17,18]. Using these methods, the SELs from M40A1 are estimated and compared with the measured values in Section 3.

2.2. Measurement description

The M40A1 recoilless rifle chosen to be measured has been developed primarily as an antitank weapon. The specifications of M40A1 and its cartridge are shown in Table 1.

"Recoilless" means that little recoil is transmitted to the operator of the weapon when the firearm is firing. This is a remarkable characteristic of M40A1 compared to other firearms. A careful examination of the weapon reveals that there is a nozzle on its tail and numerous circular holes are arranged in a zigzag pattern on its cartridge case, as shown in Fig. 2. This allows the weapon to be recoilless by exhausting combustion gas through these holes and the nozzle consecutively.

The acoustic pressure signals of the sound field were measured at a domestic military training field for a single shot with a small positive elevation angle. Microphones were deployed 1.5 m above the ground in a half-circle with a radius of 40 m according to a guideline recommended by ISO [20]. Five microphones were placed at 45° intervals around the firing point with respect to the line of fire because axisymmetry can be assumed.

Bruel and Kjaer (B&K) hand-held sound analyzers type 2250 equipped with half-inch free-field microphones were used to measure the acoustic pressure signals at the measurement points. They were oriented parallel to the ground, and their diaphragms were perpendicular to the ray extending from the source to the microphone. The ground was mostly covered with grass, sand and some bushes. The sampling frequency of the instruments was 16 kHz. Thus, their sampling interval was 62.5 μs.

3. Results and discussions

3.1. Measurement

Fig. 3 shows the acoustic pressure signals that were experimentally measured at positions of 0°, 90°, and 180° from the line of fire. In terms of the expected characteristics, these results seem to be unusual. Acoustic signals resulting from muzzle blast generally show similar waveforms regardless of the measurement position. Overpressure across a shock front is first observed and followed by relatively small rapid changes in the acoustic pressure that last for a certain period of time. This is because the sound field from weapons develops primarily by blast waves generated at the muzzle.

Table 1
Specification of M40A1 and its cartridge [16,19].

Type	Recoilless rifle		
Caliber (mm)	105		
Gross weight (kg)	113.9 (rifle, combat order)		
Length (m)	3.404		
Maximum range (m)	6900		
Muzzle velocity (m/s)	503		
Cartridge (M344A1)	Type		HEAT
	Propelling Charge		M26
	Weight (kg)	Gross	16.89
		Projectile	7.71
	Length (cm)		99.85

However, the waveforms obtained in this study differ from each other in detail. For instance, directional variation appears in the peak overpressure values. The directivity originates at the moment when the shock wave resulting from the explosion of the propellant in the barrel is discharged through the muzzle. The shock wave propagating inside the barrel is released into the firing direction, and consequently, expansion waves are formed near the muzzle because of pressure gradients with the atmosphere. Therefore, the strongest blast wave propagates into the firing direction, and it weakens progressively with angular distance from the line of fire [1]. Hence, the weakest wave propagates opposite to the firing direction. Further, the degree of directivity is related to the explosive power. As the power increases, the pressure inside the barrel and the strength of the blast wave increase, so the muzzle flow is intensely affected by the expansion waves. Typically, as the caliber of the weapon increases, more remarkable directivity patterns appear because the explosive power is greater. Therefore, the directivity pattern should be biased toward the firing direction because M40A1 is classified as a medium-large firearm depending on its caliber [21], but the measured result seems to show an unbiased pattern. This result is inconsistent with the expected characteristics, as described above.

Furthermore, the fact that the waveforms measured at different locations differ from each other is another characteristic that differs from the general features of muzzle blast mentioned previously. Microscopically, acoustic waves that seem to be a type of shock wave are discovered several times, but macroscopically, it cannot be said that they are similar because they appeared at different instants. Further, it can be said that these results are similar to those from multiple shots, as described in Fig. 4, instead of a single shot. Particularly, a comparison of the signals measured at 0° and 180° reveals that the amplitude of the pressure fluctuation that follows the blast waves at 180° is much greater than that at 0°. In terms of the similarity, this does not make sense because the weakest acoustic wave propagates opposite to the firing direction.

On the basis of these results, it could be assumed that the sound field from M40A1 is influenced by multiple sources including muzzle blast. Although reflecting surfaces such as barriers and structures that are located around the test ground could affect the sound field as sources, the lack of correlation between the signals shown in Fig. 3 supports the suggestion that there might be at least one additional source and it exhibits slightly different acoustic properties from the muzzle blast. Since the sound field by multiple sources is identical to the superposition of the individual sound fields by each source, the existence and characteristics of the additional source(s) are investigated in the following sections by examining the measurement results using several techniques such as the correlation function and Fourier transform. In addition, the type of additional source(s) is proposed according to its properties.

3.2. Temporal approaches

The major feature of the sound field by M40A1 is the fact that the waveforms measured at each position seem to be completely different from each other, as shown in Fig. 3. Nevertheless, if there was another source(s) and the sound field was superposed with that from this source(s), similar waveforms should be observed in every signal. Let us examine the two signals at 0° and 180° more closely.

Fig. 5 shows the acoustic pressure signals measured at 0° and 180° in this study. As expected, similar waveforms enclosed by double-dotted boxes were discovered in both signals with a little time-lag, which provides a clue to ascertaining the location of the additional source. When the time-lag shown in Fig. 5, which seems to be approximately 19 ms, and the corresponding distance

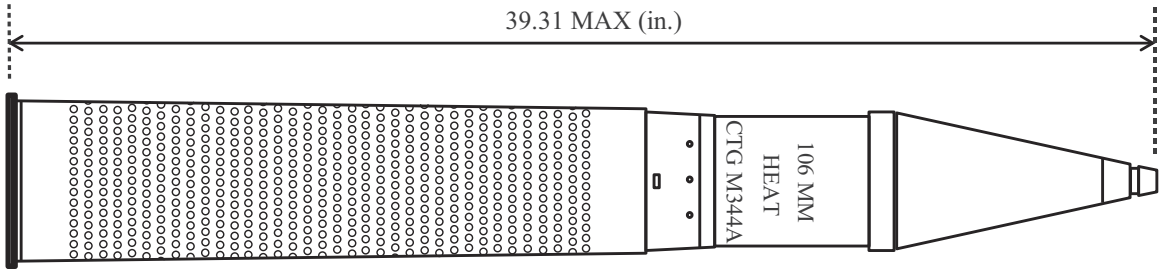

Fig. 2. Numerous circular holes on cartridge's case for M40A1 [19].

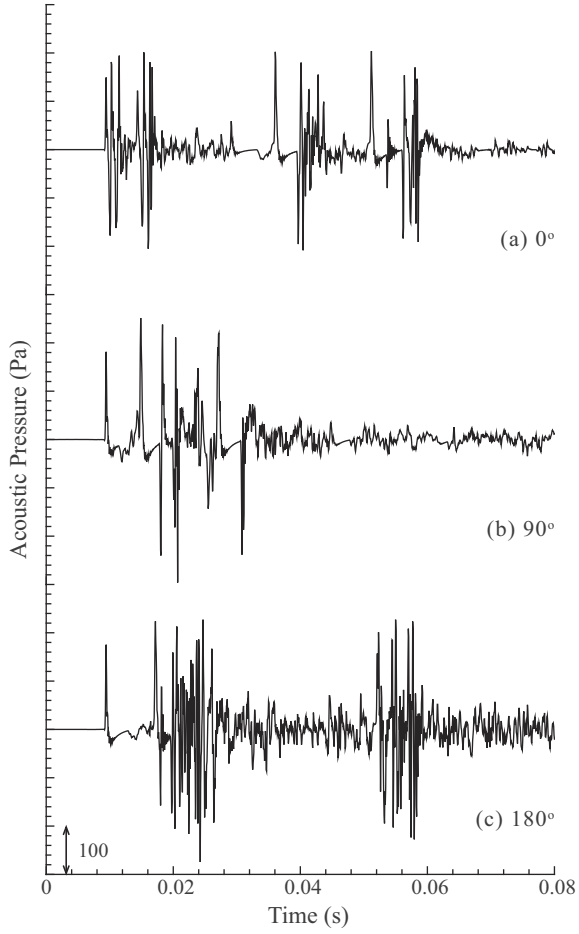

Fig. 3. Acoustic pressure signals measured in this study at the position of (a) 0° (b) 90° and (c) 180° during 80 ms.

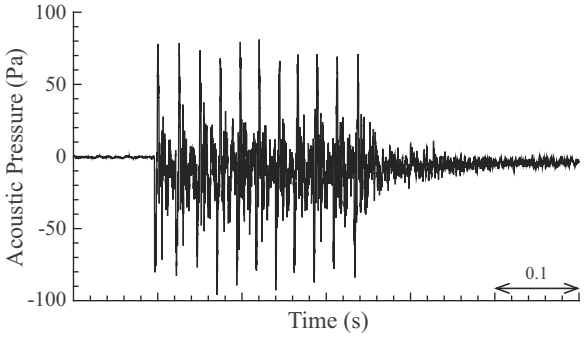

Fig. 4. Acoustic pressure signal at 25 m away from the muzzle of M167 Vulcan Air Defense System (VADS) with consecutive 10 shots.

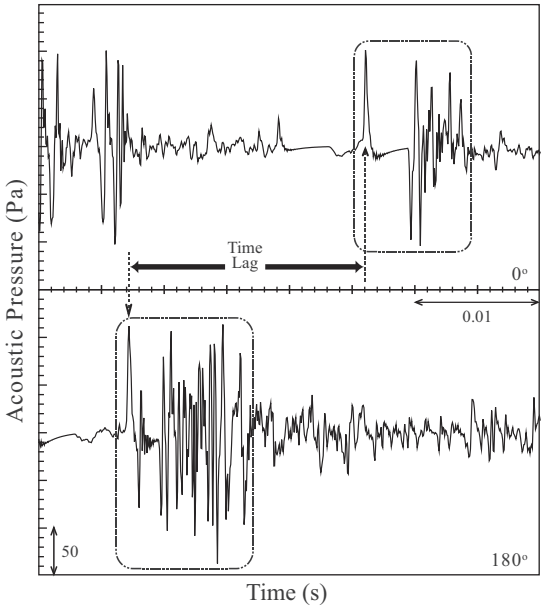

Fig. 5. Comparison of waveforms observed in acoustic pressure signals at 0° (upper) and 180° (lower).

are considered, they are thought to be practically identical to the distance gap between two potential paths from the additional source to the microphones at either 0° or 180°. If the acoustic wave might propagates at the normal speed of sound, 340 m/s, the gap is about 6.5 m, and consequently, it corresponds to the difference between the propagation paths from the rear nozzle of the firearm to both microphones. This is described in Fig. 6. This is significant evidence for the previous assumption, which implies that the extra force induced by the combustion gas exhausted through the rear nozzle would equilibrate the recoil force and make the weapon recoilless. As a result, it acts as the additional source. This can be verified using the auto- and cross-correlation functions between these signals [22].

Fig. 7(b) and (c) are two cross-correlation functions. A cross-correlation function, which indicates the degree of correlation between two real signals, has a significant value if they show similar waveforms. Fig. 7(b) describes the cross-correlation function for signals from a typical muzzle blast as shown in Fig. 7(a), and significant variation occurs at zero time-lag in this figure. Blast waves composed of similar waveforms are observed with little time-lag, and this can be interpreted as a single source of impulse sound dominates the formation of the sound field.

However, in Fig. 7(c) that describes the cross-correlation function resulting from the two acoustic pressure signals for M40A1 at 0° and 180°, which are shown in Fig. 3(a) and (c), there are two periods that have weak variations instead of a strong correlation as in Fig. 7(b). That means waveforms making up the two signals are

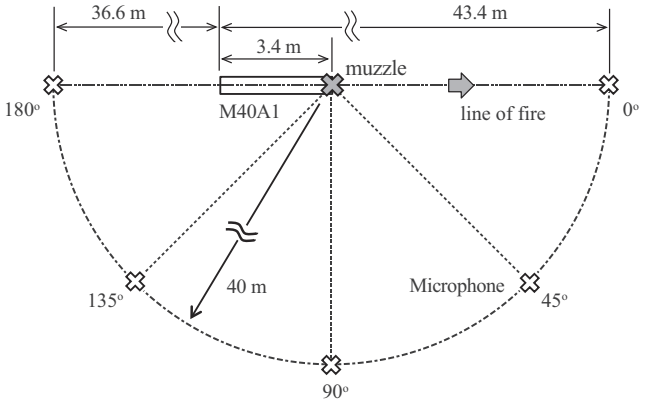

Fig. 6. Configuration of the weapon and microphones.

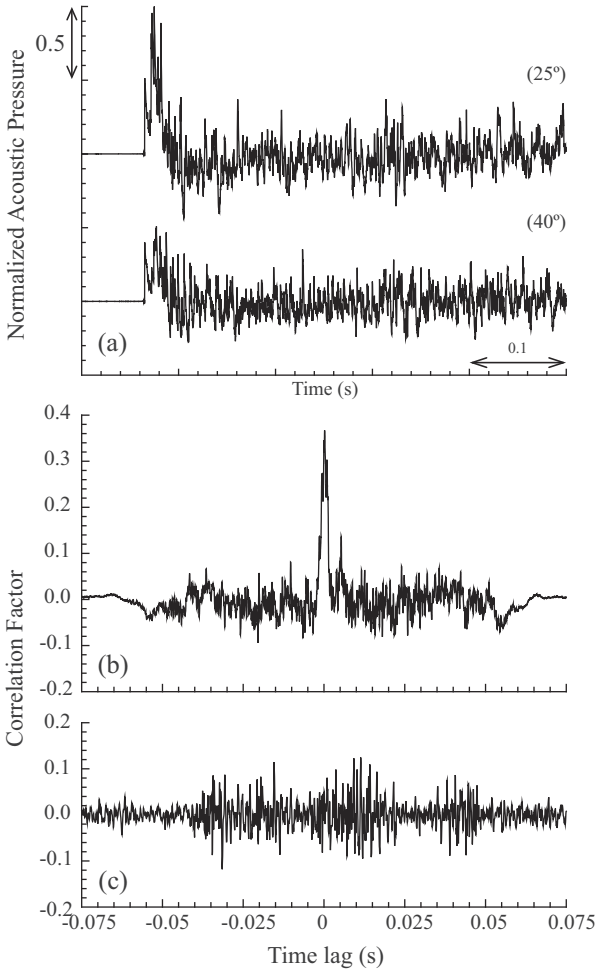

Fig. 7. (a) Normalized acoustic pressure signals from typical muzzle blast, and normalized cross-correlation functions derived from (b) signals of Fig. 7(a) and (c) M40A1 recoilless rifle.

weakly correlated for a specific range of the time-lag. Moreover, a possible interpretation is that the signals measured at different locations were not primarily influenced by the source generated at the muzzle. The weak variation occurring over 10–20 ms in Fig. 7(c) corresponds to the specific time-lag in Fig. 5. Consequently, it is possible to conclude that an additional source having similar properties is located near the rear nozzle of the weapon and significantly affects the formation of the sound field.

3.3. Spectral analysis

By using temporal analyses, it is inferred that one of the additional sources is located at the rear nozzle and affects the sound field simultaneously with the muzzle blast. In this section, spectral analysis is used to characterize the additional sources.

The frequency spectra at 0° and 180° are described as a one-third octave band in Fig. 8(a). A large amount of acoustic energy from muzzle blast is generally concentrated in low-frequency range. For instance, the peak of the amplitude spectrum can be shown to occur at f_p (Hz) = $1/2\pi c$ for a Friedlander waveform, and it is approximately 160 Hz in this study with $c = 0.001$, which was acquired by the definition of the A-duration from the measured signals of M40A1 [2]. Both results in Fig. 8(a) show similar spectral distributions over a low-frequency range with the ideal spectrum of a Friedlander waveform. The maximum amplitude values are observed at around 100 Hz in both positions, and the amplitude for each band tends to decrease as the frequency band moves toward high frequencies. However, the distributions over a high-frequency range differ from each other. Particularly, the amplitude for each frequency band at 180° shown as gray bars is obviously higher than that at 0° shown as black bars at frequencies greater than 1 kHz. According to the existence of the additional sources verified in the previous section, these level differences seem to come from these sources.

In Fig. 8(b), the measured spectra converted from the one-third octave band to the octave band are compared with the estimated spectra that were obtained by the ISO standard under the same conditions as the experiment. Similarly, typical spectral distributions that resemble that of a Friedlander waveform are predicted at both 0° and 180°, as expected. That means the ISO standard is appropriate for predicting the sound field induced by the impulse. However, the estimated spectra rarely coincide with the measured spectra from a practical viewpoint. For the results at 0° drawn as

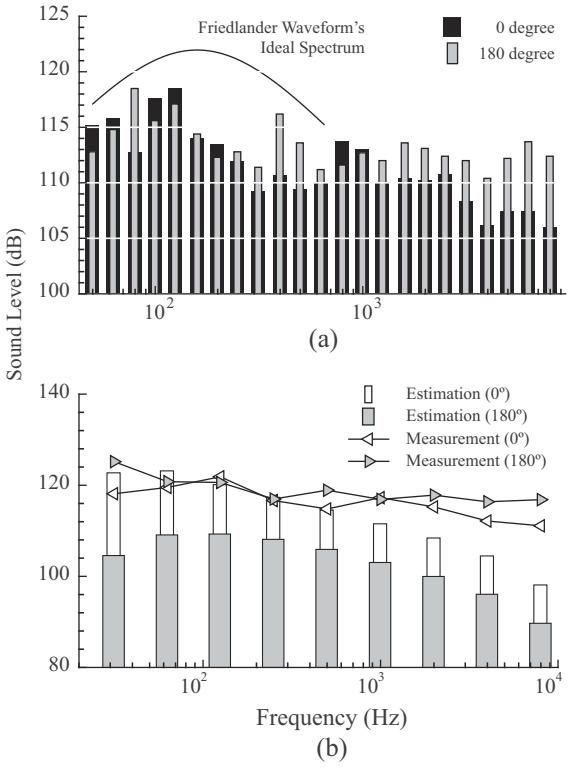

Fig. 8. Frequency spectrums: (a) measured spectrums at 0° and 180°, and (b) comparison of spectrums measured in this study and estimated by ISO standard [5,6] at 0° and 180°.

white symbols and bars, although the low-frequency components agree moderately well with each other, there are slight differences in the sound level over high-frequency range. Furthermore, remarkable disagreements occur at both low-frequency and high-frequency ranges for the results at 180° shown as gray symbols and bars.

From a slightly different perspective, the disagreement in the sound levels in Fig. 8(b) seems to result from the effects of the additional sources, which were not included in the ISO standard. At first, at high-frequency range, the fact that level differences between the measured and estimated spectra are observed at both 0° and 180° indicates that an additional source whose acoustic energy is concentrated over high-frequency range has a dominant influence on the sound field. This agrees with the fact inferred from Fig. 8(a). In addition, the fact that the differences between the measured and estimated levels at the backward are greater than those at the forward by approximately 10 dB indicates that the additional source shows a strong directivity to the backward. Furthermore, the level differences observed over low-frequency range at 180° are affected by another additional source that possesses its acoustic energy in the lower bands in the same manner. As a result, we conclude that two additional sources with peak spectral amplitudes at low- and high-frequency range, respectively, independently affect the sound field from the rear nozzle of the weapon. If the operating conditions of M40A1 are taken into account, blast noise generated when the compressed propellant gas was instantly exhausted from the rear nozzle and jet noise successively produced by the high-speed unsteady jet plume are consistent with the characteristics of the predicted additional sources.

3.4. Directivity patterns

Fig. 9(a) shows the directivity patterns for the overall SEL. The solid line with black lower triangles indicates the pattern acquired from the measured results from M40A1 and the solid line with white upper triangles is the distribution estimated by the ISO standard under the same conditions as in the experiment according to the specifications of the weapon. As this figure shows, the estimated pattern indicates the common characteristics of the muzzle blast mentioned previously. The majority of the acoustic energy is emitted into the firing direction from the muzzle, and consequently, the sound level at the forward is more than 10 dB higher than that at the backward.

However, the measurement disagrees with the estimation. The acoustic energy from M40A1 is almost uniformly discharged into all directions, but a weak directivity is observed in the backward direction. This disagreement means that the rear blast noise and jet noise at the nozzle, which were previously inferred as additional sources, affect the sound field from M40A1 simultaneously with the front blast noise at the muzzle. Further, the measured pattern suggests the extent of the influence of jet plume on the sound field. Since the unsteady jet plume from M40A1 results from the discharge of the compressed gas generated by the explosion of the propellant, equivalence to jet noise from a solid rocket engine is applicable. The directional characteristics of various types of jet noise are described in Fig. 9(b), and the directivity of a standard chemical rocket is the greatest into the angle of about 130° relative to the line of fire in this case. If the strength of the additional blast noise at the rear nozzle is the same as that of the front blast, a directivity pattern that is biased in the backward direction, like the measured results in Fig. 9(a), could be observed from only two blast sources, considering the distances between the sources and microphones. Thus, it seemed that the influence of the unsteady jet plume from M40A1 on the directional characteristics is not much substantial, as expected. In the following section, a hybrid model that includes the effects of each source is proposed to predict the sound field from M40A1, and the influence of the additional sources at the nozzle is examined according to the predicted results.

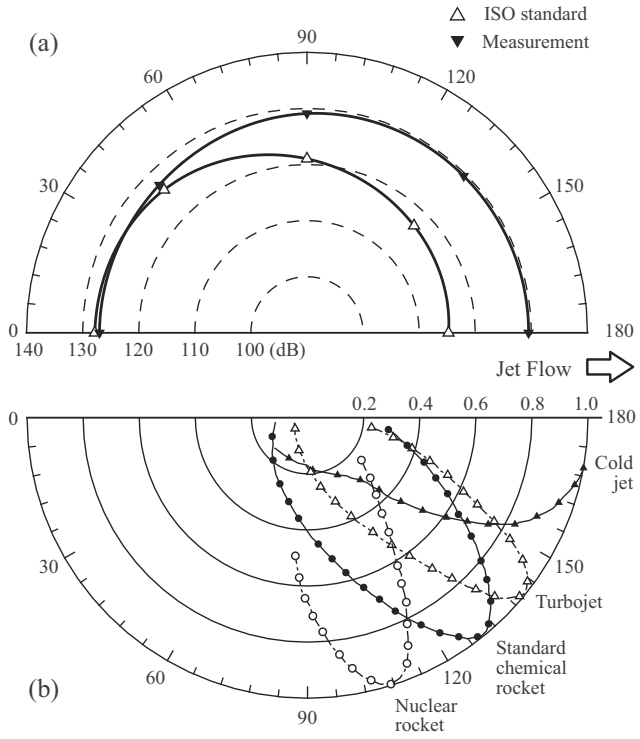

Fig. 9. Comparison of directivity patterns (a) for the measured (black lower triangles) and estimated by ISO standard (white upper triangles), and (b) those for four types of jet flow in normalized rms-pressure [23].

4. Hybrid prediction model

On the basis of the results acquired from several analyses, a hybrid prediction model is proposed to predict the sound field from M40A1 recoilless rifle. Blast noise as predicted by the ISO standard procedure is combined with jet noise predictions from the empirical formula established by NASA [23]. Finally, to verify the applicability of the hybrid model, the sound field from M67, another recoilless rifle with a 90 mm caliber, was estimated and compared with experimental results. The specifications of M67 and its cartridge are shown in Table 2 [16].

4.1. Jet noise: NASA empirical formula

The empirical method can predict the acoustic loads due to the propulsion system in terms of allocated-sources along

Table 2
Specification of M67 and its cartridge [16,19].

Type	Recoilless rifle		
Caliber (mm)	90		
Gross weight (kg)	16.4 (rifle, empty state)		
Length (m)	1.35		
Muzzle velocity (m/s)	213 (with HEAT cartridge)		
Cartridge (M371A1)	Type		HEAT
	Propelling Charge		M82
	Weight (kg)	Gross	4.16
		Projectile	3.06
	Length (cm)		70.56

the exhaust-flow axis. This method evaluates the overall acoustic power, W_{OA}, for the entire jet flow in terms of the thrust, F, exit velocity of the jet, U_e, the number of nozzles, n, and efficiency of noise generation to be one percent, and subsequently, the acoustic power spectra for each allocated-source are empirically estimated from the overall power.

$$W_{OA} = 0.005nFU_e \tag{3}$$

In Eq. (3), although the thrust is a significant parameter for evaluating the acoustic power, it is not easy to acquire the relevant information because M40A1 is not a real rocket engine. Accordingly, the thrust is defined as the force that accelerates the projectile and is calculated from a simple motion equation assuming that the projectile reaches launch speed with a constant acceleration. As a result, the thrust induced by the unsteady jet plume from M40A1 is expected to be approximately 390 kN. In addition, the core length, x_t, of the jet flow is also used as another significant parameter. Although an empirical formula for the core length was recommended by NASA, follow-up research by Varnier clarified that the core length was overestimated by the NASA model. Therefore, a modified expression in terms of the exit-nozzle diameter, d_e, and exit-nozzle Mach number, M_e, is used in this study [24].

$$\frac{x_t}{d_e} = 1.75(1 + 0.38M_e)^2 \tag{4}$$

In Eq. (4), the exit-nozzle diameter was assumed to be equivalent to the caliber of M40A1, and the Mach number was obtained by converting the exit velocity using the speed of sound at the exit-nozzle, which was calculated in terms of the specific heat ratio and temperature obtained from information on other weapons, 1.24 and 2000 K, respectively [1]. Once the core length was evaluated, a sufficient number of point sources were aligned along the jet flow. Twenty sources were allocated at constant intervals over five times the core length from the rear nozzle. As a result, the directivity patterns were acquired as the overall sound levels and are shown versus the exit-nozzle Mach number in Fig. 10. As might be expected, the most intensive directional characteristic is estimated at 135° relative to the line of fire. This is in accordance with the patterns in Fig. 9(b). In particular, since the level differences due to Mach number variation are not more than 2 dB, it can be assumed that the Mach number has little influence on the predicted results. Then, the Mach number at the exit-nozzle was assumed to be 2.5 in this prediction.

4.2. Results from the hybrid model

The sound fields resulting from the unsteady jet plume and muzzle blast, which are predicted by the empirical method and the ISO standard, are superimposed. The total acoustic energy of blast noise is assumed to be equally distributed to the muzzle and rear nozzle. As a result, a directional characteristic is obtained, as shown by the black circles in Fig. 11(a). According to this result, the directivity toward the rear of the weapon seems to be more accurate than that predicted by the ISO standard. This change comes from the influences of the additional sources originating at the rear nozzle as mentioned previously. When the overall shape is examined, it is slightly biased toward the backward direction. Although it was expected that the unsteady jet plume could cause the sound field to be significantly unbalanced, it weakly affected the sound field. That means blast sources located at the muzzle and rear nozzle induced dominantly the sound field from M40A1 because the acoustic strength of the jet plume seems to be much lower than that of the muzzle blast. In addition, the lowest sound level is estimated near the side of the weapon because no significant directional source toward 90° exists. Fig. 11(b) compares the relative directivity pattern from the measurement by Shomer et al. [25] with that measured in the present study. Although the sound levels in the forward region differ slightly, the estimated result of the hybrid model seems to agree with the measurement.

The influences of the decomposed sources can be clarified by their contribution to spectral distributions. Fig. 12 compares the spectra predicted by the hybrid model with those measured and those estimated by the ISO standard procedure at 0° and 180° . At 0° the hybrid model yields almost the same amplitude values as the ISO standard model for the entire frequency band. This means the sound field in the forward region is dominated by the front muzzle blast, as expected. On the other hand, the amplitudes at 180° are much higher for the hybrid model than for the ISO standard and are moderately consistent with the measured values. Although the influences of jet noise increases at higher frequencies, those of blast noise at the rear nozzle dominates the sound field. This coincides with the above expectations.

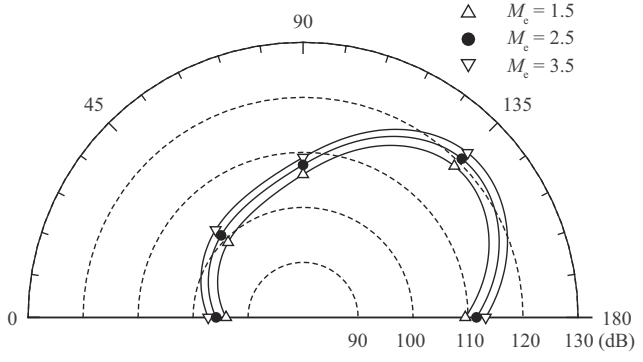

Fig. 10. Comparison of directivity patterns for unsteady jet plume estimated by the empirical formula with exit-nozzle Mach number variations 1.5 to 3.5.

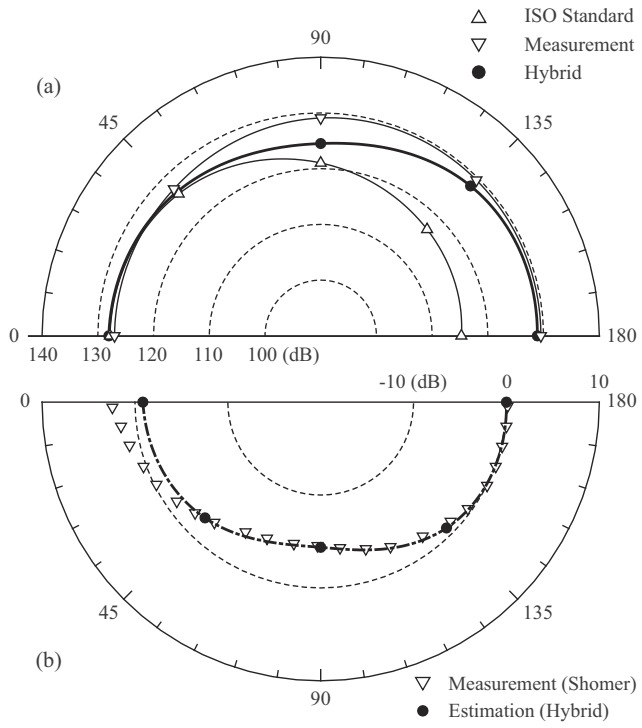

Fig. 11. Comparison of directivity pattern estimated by the hybrid model (black circle) (a) with measurement in the present study and ISO standard as overall sound levels and (b) with measurement by Shomer et al. [25] (lower triangles) as relative levels to 180°.

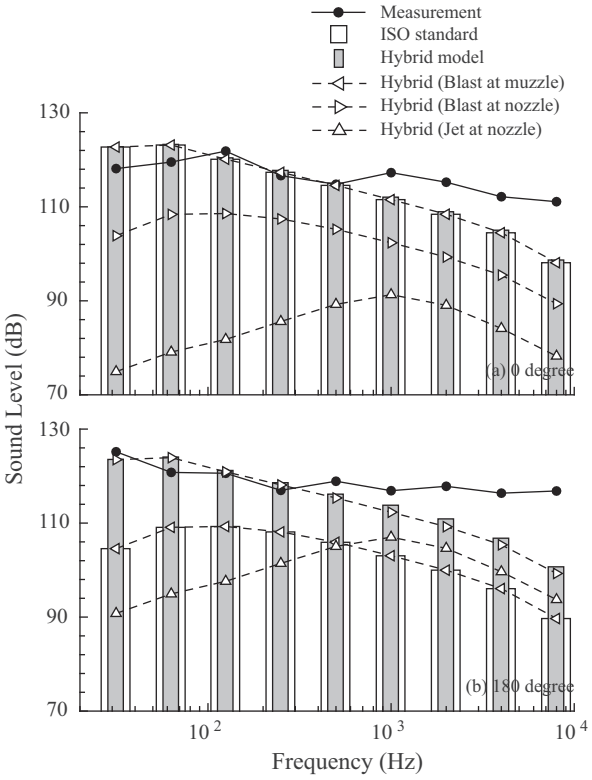

Fig. 12. Comparison of spectrums measured (black circles) and estimated by both ISO standard (white bars) and the hybrid model (gray bars) at (a) 0° and (b) 180°.

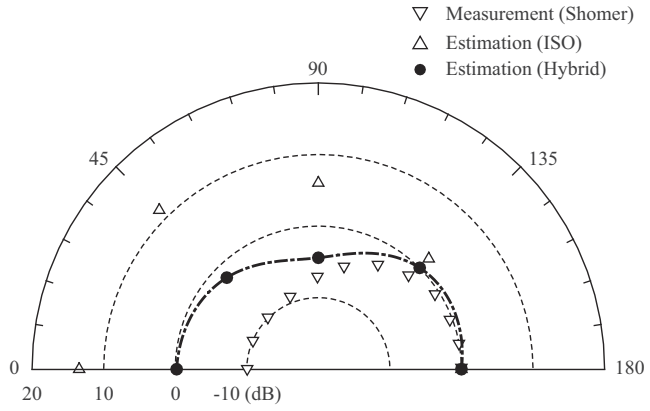

Fig. 13. Relative directivity patterns of another recoilless rifle, M67, from measured ones by Shomer et al. [25] (lower triangles) and estimated by ISO standard (upper triangles) and the hybrid model (black circles).

Finally, Fig. 13 compares the relative directivity pattern of M67 measured by Shomer et al. [25] with those estimated by the ISO standard and the hybrid model. As described before, the ISO standard yields a strongly biased distribution in the firing direction because it considers only the front blast source at the muzzle. However, although there is a slight disagreement in the forward region, the overall shape estimated by the hybrid model is closer to the measurement than the ISO standard. The results for M67 seem to be more intensely affected by the unsteady jet plume than those for M40A1. If the properties of the exhaust-flow including the unsteady jet plume are provided, the estimated results for M40A1 and M67 can be improved and become closer to the measured results.

5. Conclusion

In the present study, the characteristics of the sound sources of M40A1 recoilless rifle were investigated by analyzing the acoustic pressure signals measured when it was firing. The waveforms of the measured signals differ significantly with the measurement location, and this seems to be caused by additional source(s) that exists in addition to the blast noise at the muzzle. Based on this assumption, the measured results were examined from temporal, spectral, and directional perspectives, and two additional sources were identified at the rear nozzle of the weapon. When the operating conditions of the recoilless rifle are considered, the sources are consistent with blast and jet noise, and a hybrid prediction model integrating the influences of these additional sources was proposed. The directivity patterns and spectral distributions produced by the hybrid model indicate that it can predict the sound field from recoilless rifles more precisely than the ISO standard. It is expected that the model could be improved by future studies related to interior and transient ballistics.

Acknowledgements

This work was supported by the Human Resources Development program (No. 20124030200030) of the Korea Institute of Energy Technology Evaluation and Planning (KETEP) grant funded by the Korea government Ministry of Trade, Industry and Energy. In addition, this research was also supported by Basic Science Research Program through the National Research Foundation of Korea (NRF) funded by the Ministry of Education (NRF – 2013R1A1A2011462).

References

[1] Klingenberg G, Heimerl JM. Gun Muzzle Blast and Flash, Prog Astronaut Aeronaut 1992;139 [chapter 1, 3, 5].
[2] Hamernik RP, Hsueh KD. Impulse noise: some definitions, physical acoustics and other considerations. J Acoust Soc Am 1991;90(1):189–96.
[3] Weber W. Das Schallspektrum von Knallfunken und Knallpostolen mit einem Beitrag über die Anwendungsmöglichkeiten in der elektroakustischen Meßtechnik. Akustische Z 1939;4:377–91.
[4] Hirsch KW. On the influence of local ground reflections on sound levels from distant blasts at large distances. Noise Control Eng J 1998;46(5):215–26.
[5] ISO/FDIS 17201–2. Acoustics – noise from shooting ranges – Part 2. Estimation of muzzle blast and projectile sound by calculation. International Organization for Standardization; 2005.
[6] ISO/FDIS 17201–3. Acoustics – noise from shooting ranges – Part 3. Guidelines for sound propagation calculations. International Organization for Standardization; 2008.
[7] Fansler KS, Thompson WP, Carnahan JS, Patton BJ. A parametric investigation of muzzle blast. U.S. Army Research Laboratory ARL–TR–227; 1993.
[8] Fansler KS. Description of gun muzzle blast by modified ideal scaling model. U.S. Army Research Laboratory ARL–TR–1434; 1997.
[9] Schmidt EM, Shear DD. Optical measurements of muzzle blast. AIAA J 1975;13(8):1086–91.
[10] Bin J, Kim M, Lee S. A numerical study on the generation of impulsive noise by complex flows discharging from a muzzle. Int J Numer Methods Eng 2008;75(8):964–91.
[11] Jiang Z, Takayama K, Babinsky H, Meguro T. Transient shock wave flows in tubes with a sudden change in cross section. Shock Waves 1997;7(3):151–62.
[12] Jiang Z, Takayama K, Skews BW. Numerical study on blast flowfields induced by supersonic projectiles discharged from shock tubes. Phys Fluids 2003;10(1):277–88.
[13] Jiang Z. Wave dynamics processes induced by a supersonic projectile discharging from a shock tube. Phys Fluids 2003;15(6):1665–75.
[14] Jiang Z, Huang Y, Takayama K. Shocked flows induced by supersonic projectiles moving in tubes. Comput Fluids 2004;33(7):953–66.
[15] Erdos JJ, Del Guidice PD. Calculation of muzzle blast flowfields. AIAA J 1975;13(8):1048–55.
[16] Jones RD, Ness LS. IHS Jane's infantry weapons 2012. IHS Global Limited; 2011.
[17] ISO 9613-1. Acoustics – attenuation of sound during propagation outdoors – Part 1. Calculation of the absorption of sound by the atmosphere. International Organization for Standardization; 1993.
[18] ISO 9613-2. Acoustics – attenuation of sound during propagation outdoors – Part 2. General method of calculation. International Organization for Standardization; 1996.

[19] Technical Manual. Army ammunition data sheets for artillery ammunition: guns, howitzers, mortars, recoilless rifles, grenade launchers and artillery fuzes (federal supply class 1310, 1315, 1320, 1390). Department of the Army TM 43–0001-28; 2003. p. 5–29–30.
[20] ISO/FDIS 17201–1. Acoustics – noise from shooting ranges – Part 1. Determination of muzzle blast by measurement. International Organization for Standardization; 2005.
[21] Vos J. On the annoyance caused by impulse sounds produced by small, medium-large, and large firearms. J Acoust Soc Am 2001;109(1):244–53.
[22] Hartmann WM. Signals, sound, and sensation. New York: AIP Press; 1998.
[23] NASA Space Vehicle Design Criteria (Structures). Acoustic loads generated by the propulsion system. NASA; 1971.
[24] Varnier J. Noise radiated from free and impinging hot supersonic jets. AIAA 98-2206; 1998.
[25] Shomer PD, Little LM, Hunt AB. Acoustic directivity patterns for army weapons. U.S. Army Construction Engineering Research Laboratory CERL-IR-N-60; 1979.